Mat. Res. Soc. Symp. Proc. Vol. 791 © 2004 Materials Research Society Q5.31.1

Modeling of Deformation in Nanocrystalline Copper Using An Atomistic-Based Continuum Approach

D. H. Warner, F. Sansoz and J. F. Molinari
Department of Mechanical Engineering, Johns Hopkins University, 3400 North Charles Street, Baltimore, MD 21218 USA.

ABSTRACT

The deformation of copper with grain size less than 10 nm is investigated using a 2D continuum model incorporating atomistically-based constitutive relations. The local constitutive response of a series of symmetric and asymmetric tilt grain boundaries is obtained using an atomistic quasicontinuum method under tension and shear. The atomistic results show that it is possible to associate a constant maximum stress with each deformation mechanism triggered in the GB vicinity, i.e. GB sliding and decohesion, atom shuffling and partial dislocation emission. The GB strength is always found weaker in shear than in tension. This information is incorporated into a continuum polycrystalline model tested under compression. This model provides useful insights, in the absence of intragranular plasticity, into the onset of macroscopic quasi-plasticity, which results from GB sliding and collective grain rotation mechanisms.

INTRODUCTION

The deformation mechanisms of nanocrystalline (nc) metals at room temperature can fall into 3 categories [1,2]. First, it is possible to identify intergranular mechanisms consisting of uncorrelated atom shuffling events at high-angle grain boundaries (GB), which results in GB sliding [3,4]. Second, intragranular mechanisms such as partial dislocation emission and twinning have been observed [5-7] in nc metals with grain size larger than 10 nm. Thirdly, it has been suggested [8] that cooperative grain behaviors, i.e. microshear banding or rotation of clusters of grains may operate at this scale. An attempt is made here to develop a continuum model for the deformation of nc copper. Special emphasis is placed on modeling intergranular and cooperative grain mechanisms, hence the bulk grain behavior being treated as anisotropic elastic. In contrast to a conventional polycrystalline model, two major difficulties must be overcome at the nanoscale. One of these is the lack of understanding in the local constitutive response of GB at the nanoscale. For instance, no systematic correlations have been conducted regarding the effects of GB structures on GB-related atomic shuffling processes in previous atomistic studies of bicrystal sliding [9-11]. The second difficulty arises from treating the contact/adhesion between grains in a polycrystalline continuum model.

The local constitutive response of GB is addressed through atomistic calculations. These results are presented in the second section for 5 different GB structures tested under shear and tension. The last section presents the deformation of a polycrystalline model treated within a finite element (FEM) framework, which incorporates the atomistic-based constitutive relations obtained at GB's and allows for sliding between the grains.

COMPUTATIONAL PROCEDURE

The quasicontinuum (QC) method developed by Tadmor and co-workers [12,13], was used to simulate cells containing a bicrystal with a GB at its center. The EAM potential for copper at 0K [14] was chosen in these simulations. Non-locality was enforced across the entire GB length and within a distance from the GB plane equal to 5.25 times the potential cutoff distance (4.950 Å). All simulations were performed with less than 5000 nodes. The equilibrium structure of a GB at 0K was determined by zero force lattice statics technique [15]. The energy minimization process was conducted by a conjugate gradient method. The total energy was minimized until the addition of out-of-balance forces over the entire system was found less than 10^{-3} eV/Å. The GB energy was calculated by subtracting the single crystal energy from the bicrystal energy and dividing by the GB area. To limit surface effects in the energy calculation, only 80% of the bicrystal was considered, therefore excluding atoms near free surfaces.

The constitutive response of four <110> symmetric tilt grain boundaries (STGB) and one <110> asymmetric tilt grain boundary (ATGB) was investigated under shear and tension. The mesh was divided into 3 regions: a fixed region made of bottom atom layers, a free (unconstrained) region surrounding the GB plane and a constant-displacement region containing the top atom layers. These regions are depicted in Fig. 1. Shear and tension loading were carried out by applying a displacement parallel or perpendicular to the GB plane, respectively. The distance of atom freedom near GB was varied from 0 to 107 atom layers thick. This methodology was used to trigger successive deformation mechanisms in the GB vicinity and the crystal lattice. The dimensions of the mesh were about 383Å x 65Å and 184Å x 65Å for shear and tension, respectively. Free boundaries were imposed on the left and right sides of the mesh under shear, and the side atoms were fixed in the direction parallel to the GB under tension. All atoms were fixed in the out-of-plane direction (Z-axis) to reproduce plane strain conditions. The mean stresses were calculated as the addition of projected out-of-balance forces on top constrained atoms, and subsequently, rationalized by the GB area. General software for atomistic visualization [16] was employed for examining the central symmetry parameter [17], which provides information on the onset of planar faults during deformation.

The FEM analysis was carried out within a Lagrangian framework using a 2D plane strain explicit dynamic code. A complete description of the methodology may be found in [18]. A square sample consisting of 285 grains with a mean grain size of 10 nm was obtained by Voronoi tessellation. The mesh employed 6 node triangular elements. A texture having a <110> out-of-plane direction was considered while the in-plane crystal orientations were assigned randomly. Due to the lack of dislocation activity in copper grains smaller than 10 nm [19], each crystal was modeled as being anisotropic elastic. Stiffness coefficients corresponding to this material were taken as follows: C_{11} = 168.4 MPa, C_{12} = 121.4 MPa, C_{44} = 75.4 MPa. The bottom of the mesh was fixed in the loading direction and the bottom left corner node was fixed in the direction perpendicular to the loading axis in order to prevent translation. The sample was loaded under quasi-static compression by assigning a constant velocity to the top nodes.

The details of the contact/adhesion methodology are given hereafter. Contact and adhesion between grains was enforced at each boundary node with the contact surfaces assumed to be linear between nodes. Adhesion at each boundary node was imposed using two independent stress criteria, one for shear and the other for decohesion. The stress state at each node was defined by mapping the stresses at nearby quadrature points. In order to increase

efficiency, the microstructure was meshed so that boundary nodes of neighboring grains were coincident and could be treated as single nodes, until the critical stress criteria at the interface was met. Contact between grains was enforced using the balanced master slave approach [20]. Adhesion was implemented using a similar numerical methodology as the contact subroutine. It was applied such that coincident nodes were completely adhered until the critical stress criteria for decohesion was reached. As a first approximation, after the criteria for decohesion was met at a node, adhesive forces were no longer applied to that node throughout the remainder of the calculation.

LOCAL CONSTITUTIVE RESPONSE OF GB FROM ATOMISTIC

The shear stresses of a Σ9(221) STGB undergoing applied shear displacements are given in Fig. 1. This figure shows that the constitutive response of this boundary reaches a maximum stress after a shear displacement less than 1Å. The maximum shear stress, however, strongly decreases when the number of free atom planes near GB is increased as shown in Fig. 2a. This figure also reveals that the maximum shear stress presents 3 different plateaus, equal to 5.3, 3.5 and 1.6 GPa, corresponding to different stages of atomic freedom. From our calculations, different deformation processes are triggered during each stage. In stage I, it appears that the grains slide relative to one another with no atom shuffling at the boundary. In stage II, however, stick-slip events occur and several atom shuffling processes were observed. In tension (not shown here), there is no evidence of stage II plateau in the maximum stress; the level of stress varying progressively from stage I to stage III and no atom shuffling being observed. Finally, in stage III corresponding to relatively important distance of atom freedom as seen in Fig. 2b, the decrease of GB strength results from the interplay between atom shuffling and the initiation of planar faults. These faults are evident in the form of partial dislocations emanating from sites left free after atom shuffling.

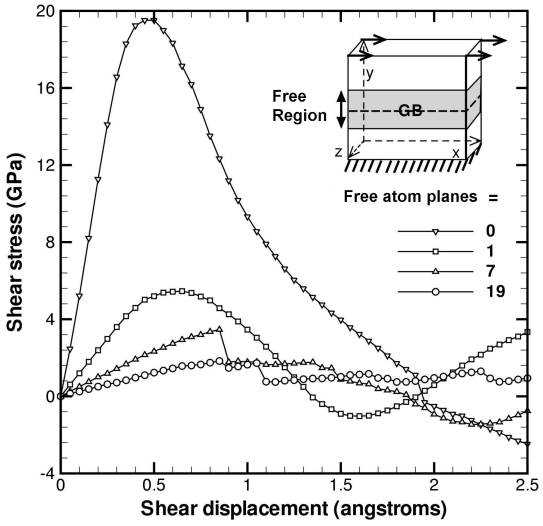

In conclusion, it may be thought that, in tension, GB act as partial dislocation sources accelerating crystal damage and GB-related atom shuffling has a limited role in this mode, while, in shear, shuffling is the predominant factor responsible for the decrease of boundary strength and the presence of an intermediate plateau in maximum stress. Therefore, since our objective is to distinguish the intrinsic GB strength from crystal plasticity effects, the local constitutive response of a Σ9(221) STGB is found from the shear stress measured in the stage II plateau for shear (3.47 GPa) and the tensile stress measured in the stage I plateau for tension (15.4 GPa).

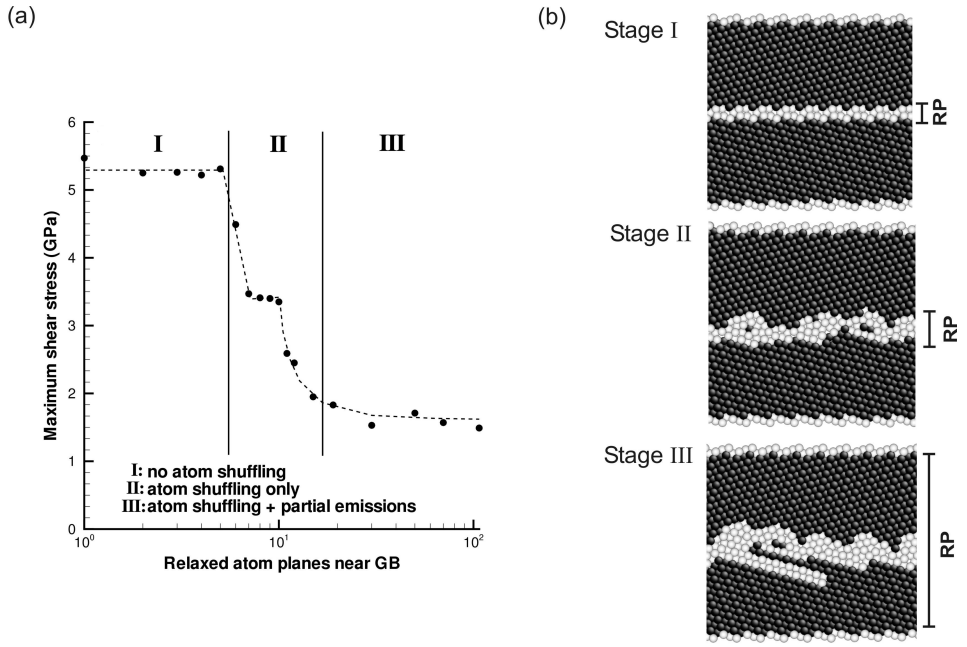

Figure 2. (a) Maximum shear stress versus number of free GB planes in Σ9(221) symmetric tilt grain boundary. (b) Partial view of the same GB after the maximum shear stress is reached with different atomic freedom. Atoms in dark color are perfect fcc crystal stacking. Atoms in bright color are planar faults. RP is the distance between which atom planes are free.

The maximum shear stress in stage II and stage III are compared in table I for 5 different GB structures. It is important to note in this table that boundaries, which do not promote atom shuffling, have no stage II plateau. This is observed when the GB energy is below 570 mJ/m^2. The value of the plateau in stage III seems highly dependent upon the nature of deformation processes in the GB region. However, the plateau in stage II is always found near 3.5 GPa regardless of the GB structure. A grain boundary undergoing atom shuffling can therefore be modeled with the same local constitutive response.

Table I. Effects of GB structure on the maximum shear stress and deformation mechanisms. STGB = symmetric tilt grain boundary, ATGB = asymmetric tilt grain boundary.

GB type	Energy (mJ/m^2)	Maximum shear stress (GPa) Stage II	Stage III	Stage III mechanisms
Σ9(221) STGB	833	3.47	1.53	shuffling + partials
Σ9(552)/(771) ATGB	745	3.61	1.62	shuffling + partials
Σ27(115) STGB	700	3.23	3.14	shuffling only
Σ33(554) STGB	570	no shuffling	2.38	GB migration + partials
Σ11(113) STGB	307	no shuffling	5.87	partials only

POLYCRYSTALLINE DEFORMATION

In the polycrystalline modeling, a thermal correction which is based on molecular dynamics simulations of nc copper from 0K to 300K [21], was performed on the 0K stress value obtained above. Therefore, a constant value of 2.3 GPa was used as the critical resolved shear stress (CRSS) necessary to shear a grain boundary and 11.5 GPa was taken as the necessary tensile stress to obtain separation of the boundary. The sample was tested up to 5% compression.

GB sliding processes occur after a macroscopic deformation of 2.3% as shown in Fig. 3. As compared to specimens without GB sliding, these processes are found to increase the magnitude of stress heterogeneity for the same applied deformation. Throughout the following 0.5% strain a decrease in the stiffness of the sample is obtained and sliding occurs in most of the grain boundaries except those with weak orientation with respect to the loading axis. At a deformation of 2.8%, a sharp decrease in stress is measured coinciding with the formation of voids/microcracks. Subsequently, there is a regime, in which the stress increases due to the lack of GB sliding, which is enforced by geometrical locking. This regime stops when the level of stress is high enough to nucleate a void in the microstructure. Void nucleation reduced the global stress and allowed for more sliding to occur. This process seems to repeat itself due to further geometric locking. Throughout these cycles, collective grain rotation is observed as reported in MD calculations [2].

CONCLUSIONS

The local constitutive response for different GB structures was obtained by atomistic calculations on copper bicrystals under tension and shear. These results show that the maximum GB strength and the nature of deformation processes highly depend upon the extent of atom freedom in the GB vicinity. The presence of a plateau in maximum shear stress is detected when atom shuffling is triggered and no crystal plasticity effects operate. The GB constitutive response was incorporated into a polycrystalline anisotropic elastic model using FEM method.

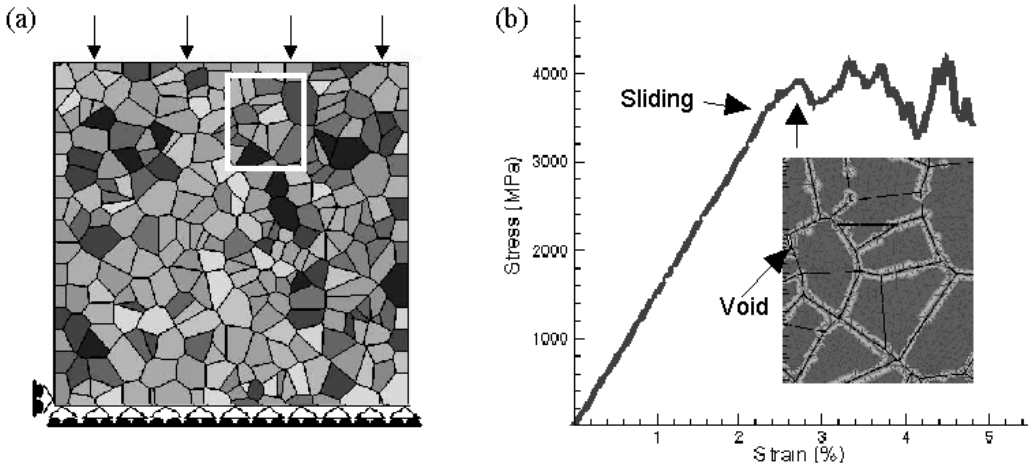

Figure 3. (a) Initial FEM polycrystal model. Grain colors denote in-plane grain orientation (b) Uniaxial stress in the loading direction versus applied strain. Magnification of the mesh after 2.7% strain showing GB sliding (highlighted) and void formation (near arrow).

Under uniaxial compression, this model reveals that GB sliding in a microstructure having no intragranular plastic deformation can produce macroscopic quasi-plasticity. Higher stress heterogeneities across the boundaries have been found in microstructures promoting sliding. These local high stresses seem to play an important role in triggering cooperative grain mechanisms. Further calculations are planned which will incorporate a non-local plasticity model to describe bulk grain behavior by taking into account the emission of dislocations from the GB.

ACKNOWLEDGMENTS

This work was performed under the auspices of NSF-Nanoscale Interdisciplinary Research Team under contract DMR-0210215 and ARL-Center for Advanced Materials and Ceramic Systems under the ARMAC-RTP Cooperative Agreement Number DAAD19-01-2-0003. We also acknowledge E. Tadmor and R. Miller for providing the QC code.

REFERENCES

1. H. Van Swygenhoven and J.R. Weertman, Scr. Mater. **49**,625 (2003).
2. K.S. Kumar, H. Van Swygenhoven and S. Suresh, Acta Mater. **51**,5734 (2003)
3. H Van Swygenhoven and P.M. Derlet, Phys. Rev. B **64**,224105 (2001).
4. K.S. Kumar, S. Suresh, M.F. Chisholm, J.A. Horton and P. Wang, Acta Mater. **51**, 387 (2003).
5. J. Schiotz and K.W. Jacobsen, Science **301**,1357 (2003).
6. M. Chen, E. Ma, K.J. Hemker, H. Sheng, Y. Wang and X. Cheng, Science **300**, 1275 (2003).
7. X.Z. Liao, F. Zhou, E.J. Lavernia, S.G. Srinivasan, M.I. Baskes, D.W. He and Y.T. Zhu, App. Phys. Lett. **83**, 632 (2003).
8. A. Hasnaoui, H. Van Swygenhoven and P.M. Derlet, Science **300**, 1550 (2003).
9. J.H. Rose, J. Ferrante and J.R. Smith, Phys. Rev. Letters **47**,675 (1981).
10. N. Chandra and P. Dang, J. Mater. Sci. **34**,655 (1999).
11. M. Grujicic, G. Cao and P.F. Joseph, Int. J. Multiscale Comp. Eng. **1**,1 (2003).
12. E.B. Tadmor, M. Ortiz and R. Phillips, Philos. Mag. A **73**,1529 (1996).
13. V.B. Shenoy, R. Miller, E.B. Tadmor, D. Rodney, R. Phillips and M. Ortiz, J. Mech. Phys. Solids **47**,611 (1999).
14. S.M. Foiles, M.I. Baskes and M.S. Daw, Phys. Rev. B **33**,7983 (1986).
15. J.D. Rittner and D.N. Seidman, Phys. Rev. B **54**,6999 (1996).
16. J. Li, Modelling Simul. Mater. Sci. Eng. **11**,173 (2003).
17. C.L. Kelchner, S.J. Plimpton and J.C. Hamilton, Phys. Rev. B **58**,11085 (1998)
18. J.F. Molinari, M. Ortiz, Int. J. Numer. Meth. Eng. **53,**1101 (2002)
19. S. Cheng, J.A. Spencer and W.W. Milligan, Acta Mater. **51**,4505 (2003).
20. L. Taylor and D. Flanagan, Technical Report SAND86-0594, Sandi National Laboratories, Albuquerque, NM (1987).
21. J. Schiotz, T. Vegge, F.D. Di Tolla, and K.W. Jacobsen, Phys. Rev. B **60**,971 (1999).